HEAT TRANSFER PERFORMANCE OF A VIBRATED TWO-PHASE CLOSED THERMOSYPHON

أداء إنتقال الحرارة لسيفون حرارى مغلق مهتز

M. A. Shalaby, G. I. Sultan and A. Abdel Salam

Mech. Power Eng. Department, Faculty of Engineering
Mansoura University, Egypt, P. O. 35516
E-mail: gisultan@mum.mans.eun.eg

الخلاصة:

تم عمل دراسة معملية لبيان أداء إنتقال الحرارة لسيفون حرارى مغلق مهتز وكان مائع التشغيل المستخدم هو R134a . تم دراسة تأثير الفيض الحرارى ($1276W/m^2 \le q \le 6331W/m^2$)، نسبة الإمتلاء ($30\% \le V^+ \le 100\%$)، والتردد الإهتزازى اللابعدى ($1.08 \le F \le 3.26$)، وسعة الإهتزاز اللابعدية ($0.19 \le B \le 0.57$) على أداء السيفون الحرارى المهتز. ووجد أن أفضل نسبة إمتلاء وتردد إهتزازى لابعدى هى 50% و 1.448 على الترتيب. وتم التوصل إلى علاقة لابعدية لرقم نوسلت كدالة فى رقم كوتاتيليدزيا ، ونسبة الإمتلاء ، ونسبة التردد اللابعدى، وسعة الإهتزازة اللابعدية وكذلك نسبة الضغط.

ABSTRACT

An experimental investigation had been carried out in order to study the heat transfer performance of a vibrated two-phase closed thermosyphon tube. The working fluid used was R143a. The effects of heat flux ($1276W/m^2 \le q \le 6331W/m^2$), filling percentage ($30\% \le V^+ \le 100\%$), the vibration dimensionless frequency ($1.08 \le F \le 3.26$), and the dimensionless amplitude ($0.19 \le B \le 0.57$) were studied. It was found that, the optimum filling percentage and the best dimensionless frequency values are 50% and 1.448 , respectively. The Nusselt number had been correlated in a dimensionless form as a function of Kutateladze number, filling ratio, dimensionless frequency, dimensionless amplitude, and reduced pressure ratio.

Keywords: Two-phase closed vibrated thermosyphon, filling ratio.

INTRODUCTION

The thermosyphon is a passive device, which is used to transfer a large amount of heat, with small temperature difference, by evaporation of the working fluid through the evaporator section and condensing it in the condenser section. In practice, the effective thermal conductivity of thermosyphon exceeds that of copper, Rosler [1987]. The thermosyphon is widely used in many energy and industrial applications. Examples include heat exchangers, solar collectors, cooling of electronic equipment, systems for the prevention of ice formation on roads, cooling of gas turbine rotor blades, preservation of permafrost in arctic regions, and extraction of geothermal energy. A considerable experimental and theoretical work had been done on the application and design modifications for improving thermosyphons performance, in case of stationary thermosyphons. Lee and Mital [1972] studied the heat transfer performance of a two-phase closed thermosyphon together with a simple theoretical analysis for its maximum heat transfer capacity. They used water and R11 as working fluids. The heat transfer in a two-phase closed thermosyphon with water and ethanol as working fluids were studied by Imura et al. [1979]. They found that the optimum filling ratio was 10-20 percent of the tube inside volume and established an empirical formula for the heat transfer coefficient in the evaporator section for a thermosyphon installed in a vertical position. Nguyen-Chi et al. [1979] investigated experimentally the performance of vertical two-phase closed thermosyphons using water as a working fluid. Shiraishi et al. [1981] studied experimentally the heat transfer characteristics of a two-phase closed thermosyphon and developed a simple

Accepted June 30, 2003.

mathematical model to predict the performance of such thermosyphons. They used water, ethanol and R113 as working fluids. Hahne and Gross [1981] performed an experimental investigation to predict the effect of inclination angle on the transport behavior of a closed two-phase thermosyphon using R115 as a working fluid . Negishi and Sawada [1983] made an experimental study on the heat transfer performance of an inclined two-phase closed thermosyphon. They used water and ethanol as working fluids. Gross and Hahne [1985] studied experimentally the effects of pressure, heat flow rate and inclination angle on the heat transfer near the critical state. They used R115 as a working fluid and found that the optimum inclination angle was about 40°. Negishi et al. [1991] studied the influences of the filling ratio and inclination angle on the heat transfer performance of a corrugated tube thermosyphon. Park and Lee [1992] made an experimental study on the performance of two-phase closed thermosyphons with three working fluid mixtures (water-glycerin, water-ethanol, and water-ethylene glycol). They found that for all values of filling ratio, the tested thermosyphon had a highest performance at an inclination angle of about 60° from the direction of the gravitational force. Gunnerson and Zuo, [1995] studied theoretically the heat transfer characteristics of an inclined two-phase thermosyphon. Shiraishi et al.,[1995] conducted a flow visualization study of the inside flow phenomena of an inclined two-phase closed thermosyphon. They used R113 as a working fluid. Terdtoon et al. [1996] investigated the effect of aspect ratio (ratio of evaporator section length to diameter) and Bond number on the heat transfer characteristics of an inclined two-phase closed thermosyphon. They used R22, ethanol, and water as working fluids, and a filling percentage of 80%. They found that the aspect ratio and Bond number did not affect the angle at which the highest heat transfer rate occurred. The heat transfer in a vertical annular two-phase closed thermosyphon had been studied experimentally with distilled water as a working fluid by Abdel-Aziz, [1996]. The effects of heat flux, liquid fill charge, and evaporator to condenser length ratio on the heat transfer coefficient, were investigated. He showed that the maximum overall heat transfer coefficient occurred at an evaporator to condenser length ratio ranged between 0.33 to 1.0, and the liquid fill charge was about 16% based on the total thermosyphon inside volume. Abou-Ziyan, et al. [2000] made an experimental study of a two- phase closed thermosyphon to predict its performance characteristics under stationary and vibrated conditions. They used water and R134a as working fluids. They investigated the effects of the filling ratio, and the length of adiabatic section on the output heat flux for a wide range of input heat flux with water as a working fluid for stationary experiment. Also, they investigated the effects of vibration on the output heat flux using water and R134a as working fluids. The frequency range was varied from 0 to 3.33 Hz. Ferguson and Lilleteht, [1996] presented a model of therm-vibrational convection in a vertical cylindrical cavity, and studied the frequency dependence of heat transfer rate through the system at several Rayleigh number, and Grashof number. Shiraishi et al., [1996] investigated experimentally the critical heat transfer rate in an inclined two-phase closed thermosyphons. They investigated the effects of the ratio of evaporator length to inner tube diameter, fill charge, working fluid property, and operating pressure. Shalaby et al., [2000] presented an experimental study on the heat transfer performance of low temperature two-phase closed thermosyphon. Their experiments were performed to investigate the effect of heat flux, filling ratio (volume of the working fluid to the evaporator volume), and the inclination angle on the performanee of low temperature two-phase elosed thermosyphon. They used R22 as a working fluid. Rosler et al., [1987] presented an experimental and theoretical investigation of heat transfer characteristics of a vertical annular closed two-phase thermosyphon. They used R113 as a working fluid. Faghri et al., [1989] studied the heat transfer in the condenser section of conventional and annular two-phase closed thermosyphon tubes experimentally and analytically. They used R113 and acetone as working fluids. They developed an improved correlation to predict the performance limits of conventional

thermosyphon flooding with different working fluids. Wang, and Ma,[1991] performed experimental and theoretical investigation for condensation heat transfer inside vertical and inclined thermosyphon. They used water as a working fluid. Peterson and Ma, [1999] presented a detailed mathematical model for predicting the temperature drop as a function of heat transfer capability in a micro heat pipe. Hideaki et al.,[1999] performed an experimental investigation on the effect of heat flux, inside pressure, type of working fluid, amount of liquid filling ratio, and the dimensions of a thermosyphone tube on the occurrence of geysering. They used water and ethanol as a working fluid. Imura, et al., [1999] performed an experimental study of critical heat flux in a double tube two-phase closed thermosyphon. They used water, R-113, and ethanol as working fluids. They investigated the effects of the tube diameter, evaporator length, working fluid, fill charge ratio, and inside temperature on the critical heat flux. Akihiro, [1999] performed an experimental study of a flexible heat pipe using acetone as working fluid. He investigated the effect of inclination angle of the condenser and heat input. The result indicated that the vibration did not affect remarkably in the performance of the flexible heat pipe. Mahgoub et al., [2000] presented an experimental and theoretical study on the flow and heat transfer performance of the two-phase offset and elbow thermosyphons. The maximum heat transfer coefficient occured at length ratio of 1.5. Ong et al., [2000] presented an experimental study on performance of a R-134a-filled thermosyphon operating at low temperatures. Casarosa et. al.,[1983] described an interesting phenomenon during their experimental work on a two-phase thermosyphon with water as working fluid. The phenomenon was pulsed boiling at low pressure. They called it "Geyser Effect". Kim et al.,[2000] presented a numerical and experimental methods for the dissipation limit under the conditions for natural convection cooling of a heat sink which has been an issue of great interest in the mobile communication industry. The effect of forced transverse vibrations on the local heat transfer of a heated cylinder near its first two natural frequencies had been studied experimentally by Murphy and Lambert [2000]. Melikeyev et al.,[2002] studied analytically and experimentally the heat and mass transfer processes in the thermal heat pipe subjected to vibrating influence. They investigated analytieally the condensation thickness of a vibrated heat pipe.

From the available literature review, one may observe that a limited number of working fluids had been used and some of them are rarely used, such as R134a. In addition to that, since most of the working engineering systems generates vibration, and the research work studying the vibration effect was also found to be very view. So, the parameters suggested, in order to study their effects on the performance of the closed two-phase thermosyphon still need more work.

The aim of the present work is focused to study the effect of some parameters on the performance of a vibrated closed thermosyphon, with R134a as a working fluid. These parameters are the heat flux, the filling ratio percentage, the vibration frequency as well as the vibration amplitude.

EXPERIMENTAL APPARATUS

Figure 1 shows a schematic diagram of the experimental apparatus. The experimental test section is shown in Fig. 2. The thermosyphon tube (4) is made of a smooth copper with 21mm inside diameter, 2-mm thickness, and 1500-mm total length. The thermosyphon consists of three sections: the lower section, 600 mm long, constitutes the evaporator, the middle section, 300-mm long represents the adiabatic section, and the third section of 600 mm long constitutes the condenser. R134a is used as a working fluid (28). The evaporator section is uniformly heated by the main electric heater (26), which is made of a nickel chrome strip (4.5 Ω/m, 3.1 mm width, and 0.2 mm thiek). Before winding the main electrical heater, the copper tube is wrapped with an insulating tape (29) along the evaporator section. The

insulating tape is made of a non-alkali fiberglass (0.13 mm thick, and 25 mm wide). The main electric heater is wound around the evaporator section at equal pitches (every 2.0 mm of the evaporator length) to introduce a constant heat flux. After winding the main electric heater, it is wrapped with an electrical insulating tape, and covered by a cylindrical insulation (30), which is made of a glass wool (40-mm thickness).

The guard heater (27) is wound over the glass wool insulation at equal pitches (every 30.0-mm along the evaporator section). The guard heater is made of a nickel - chrome strip (8.5 Ω/m, 1.5 mm wide, and 0.2 mm thick), and is used to compensate the heat losses from the main electric heater to the environment. After winding the guard heater, it was covered with glass wool insulation (10 mm thick). To prevent the heat loss from the bottom of the thermosyphon tube, it is covered with glass wool insulation (10 mm thick). The electric power input to the main heater is controlled by a variable power supply (variac) (20). The power input to the guard heater is varied until the two thermocouples T_{17} , T_{18} (which is inserted 20.0 mm apart in the glass wool between the main and guard heaters) has the same reading. The adiabatic section is covered by a cylindrical insulation, which is made of a glass wool (40 mm thick).

A number of thermocouples of type-K (Copper-Constantine) are used to measure the temperature distribution along the outer surface of the thermosyphon tube. Five of them are glued at equal spacing along the evaporator section, another four thermocouples are glued on the wall of the adiabatic section, and the last five thermocouples are glued on the condenser section. Two thermoeouples are placed at inlet and outlet water jacket of the condenser.

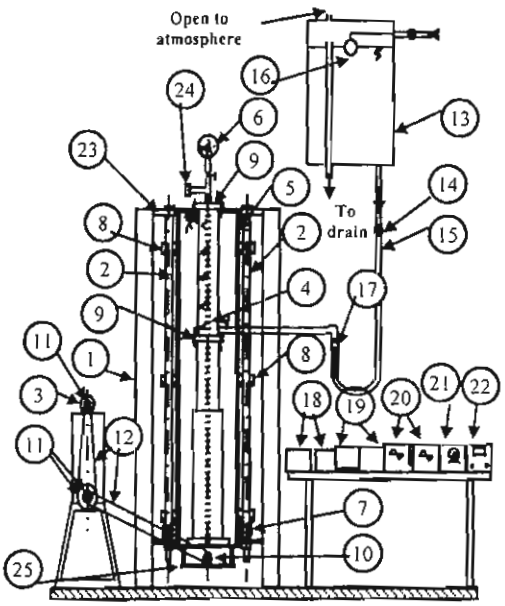

Fig. 1 Schematic diagram of experimental apparatus.

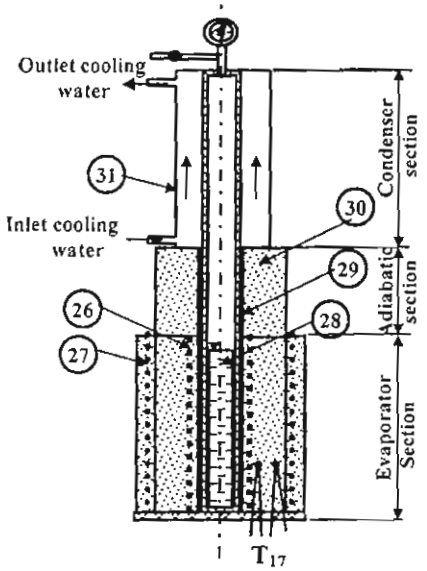

Fig. 2 The experimental test section

1. Beam [U], 2. Shaft, 3. Electrical motor, 4. Thermosyphon Tube, 5. Iron bar, 6. Pressure gauge, 7. Springs, 8. Journal Bearing, 9. Flanges, 10. Eccentric Disc , 11. Pulleys, 12. Belts, 13. Isolated Tank, 14. Gate Valve, 15. Rubber pipes, 16. Float., 17. Rotameter, 18. Voltmeters, 19. Ammeters, 20. Auto-transformers, 21. Stabilizer, 22. Temperature Recorder, 23. Outlet water, 24. Non-return valve. 25- follower, 26- Main heater, 27- Guard heater, 28-Working fluid. 29-electrical insulation tape, 30-Cylindrical insulation, 31. Water jacket.

All the thermocouples are connected to a digital temperature recorder (22), which has an inaccuracy of ± 1% of the measured value. Two auto-transformers (20) are used to change the power input to the main heater and the guard heater by the aid of two ammeters (19) and two voltmeters (18). A stabilizer (21) is connected to the two auto-transformers and the variable speed motor (3) which are used to vibrate the thermosyphon to ensure that the fluctuations in the input power is very small.

The condenser section is cooled by water that flows through an annular water jacket (31). The cooling jacket of the condenser is made of steel, 50 mm inside diameter and 600 mm length. The cooling jacket and the thermosyphon tube are assembled by two-flange (9). A two rubber O-rings are mounted at the ends of the condenser section to prevent water leakage between the cooling jacket and the thermosyphon tube. A constant level water head is obtained by using a float valve (16), which is mounted on the water inlet to the tank. The total head of the supply water is 2.5m above the cooling water inlet. All connecting tubes used in cooling water circuit are made from PVC tube (15). The flow rate is controlled by a valve and measured by a rotameter (17). The cooling water temperature is about 27C and water flow rate at 50 Lit/hr.

The vibration mechanism is consisted of an eccentric disc (10) mounted on the shaft by key. A variable speed motor (3) is used to change the vibration frequency. Two guide shafts (2), (1.5 m long), each of them is fixed with two steel pieces which are fixed on two vertical beams (1). Six bearings (8) which slide on the guide shaft (2) (three bearing on each shaft), in which the outer racing of the bearings are welded on an iron bar (5) of cross section (1cm ×1cm), the follower (25) and two springs (7). The motion is transmitted from the motor to pulleys (11) to reduce the speed and increase the torque through V-belts (12),which is mounted on the same shaft of the eccentric disc (10), which touches the follower (25). The pipe is vibrated when the follower transmits the eccentric disc motion to the pipe. The bearings are sliding on the vertical shaft against the springs (7).

CALCULATION PROCEDURE

In this research, the overall heat transfer coefficients of the thermosyphon (U), the convective heat transfer coefficient of both evaporator (h_e), and condenser sections (h_c). respectively, are defined as the following [12]:

$$U = q/(T_{e,ave} - T_{c,ave}) = 1/(1/h_e + L^+/h_c) \quad (1)$$

$$h_e = q/(T_{e,ave} - T_{a,ave}) \quad (2)$$

$$h_c = qL^+/(T_{a,ave} - T_{c,ave}) \quad (3)$$

The average Nusselt number is obtained from the relation:

$$Nu = U\, di\, /kl \quad (4)$$

RESULTS AND DISCUSSION

Experimental runs are performed to study the effect of heat flux q, filling ratio V^-, dimensionless amplitude B, and the dimensionless frequency F, on the performance of a vibrated two-phase closed thermosyphon.

In order to examine the reliability of the test rig, the present experimental results of average wall temperature versus frequency in case of 50% filling ratio and 3780 W/m^2, is compared with the corresponding published data [24], as shown in Fig.(3). It is noticed that the present experimental results of the average wall temperature, as expected, increases with

the increase of frequeney and has a good agreement with results of [24] in the range (0-3 Hz), but it must be extended to cover a large range of frequencies (up to 9 Hz) and different amplitudes.

Temperature Distribution along the Thermosyphon

Figure 4 shows the temperature distribution along the axial direction of the thermosyphon tube for the filling ratio 50%, at different heat fluxes and in case of stationary thermosyphon. It is clear that, the wall temperature along the thermosyphon tube increases with input heat flux (q). It can be observed that the temperatures increase up to x/L=0.2 from the evaporator bottom and then decreases along the evaporator section. This is because the axial conduction in the pipe wall causes the wall temperature in the adiabatic section decreases in the axial direction. The wall temperature in the condenser section increases in the axial direction because the boundary layer thickness decreases in this direction.

Figure 5 shows the temperature distribution along the thermosyphon at a heat flux q= 6631W/m^2 in a vertical position at different filling ratios and stationary thermosyphon. It is clear that the wall temperature along the thermosyphon decreases with decreasing the filling ratios. The wall temperature in the evaporator section increases and the decrease is nearly uniform. The wall temperature in the adiabatic section decreases along in the axial direction, while the wall temperature in the condenser section increases along the axial direction.

Figure 6 shows the temperature distribution along the thermosyphon tube at dimensionless amplitude of 0.285, heat flux 3780 W/m^2, 50% filling ratio, and different frequency. It is clear that the wall temperature along the thermosyphon increases with the frequency increase. The wall temperature in the evaporator section increases with the frequency increase. The wall temperature in the adiabatic section decreases upward in the axial direction and increases with the frequency, while the wall temperature in the condenser section increases upward in the axial direction, and it increases with frequency. Increasing the frequency leads to increase the vapor velocity and consequently the interfacial of liquid from the condensate film into the vapor core. This reduces the boundary layer thickness, resulting in an increase of the wall temperature.

Figure 7 shows the temperature distribution along the thermosyphon tube at dimensionless frequency of 1.448, heat flux 3780 W/m^2, 50% filling ratio, and different dimensionless amplitude. It is clear that the wall temperature in the evaporator section increases with the dimensionless amplitude increase. The wall temperature in the adiabatic section decreases upward in the axial direction and increases with the dimensionless amplitude, while the wall temperature in the condenser section increases upward in the axial direction, and increases with dimensionless amplitude.

Effect of Operating Parameter on the Temperature

Figure 8 shows the effect of filling ratio on the average wall temperature of the condenser and the evaporator sections at the heat flux of 3780 W/m^2, 0.285 dimensionless amplitude, and different dimensionless frequency. It is clear that with increasing the filling ratio the wall temperature of the evaporator and condenser sections increases.

Figure 9 shows the effect of the dimensionless frequency on the average temperature of both evaporator and condenser sections at filling ratio of 50%, 3780 heat flux, and different dimensionless amplitude. It is clear that with increasing the frequency the wall temperature of the evaporator and condenser sections increases. Figure 10 shows the effect of the dimensionless amplitude on the average wall temperature of the condenser and the evaporator sections at filling ratio of 50%, heat flux of 3780W/m^2, and different dimensionless frequency. It is clear that with increasing the dimensionless amplitude, the wall temperature of the evaporator and condenser sections increases.

Effect of the Frequency

Figure 11 shows the variation of the overall heat transfer coefficient with the dimensionless frequency at filling ratio 50%, different the dimensionless amplitude, and the heat flux 3870W/m^2. It is clear that the overall heat transfer coefficient increases with increasing the dimensionless frequency to reach the maximum value (peak point) at 1.448 (natural frequency). The effect of vibration on the thermosyphon enhances the performance by 5 to 18.8% over the range of this study. For example, at V^+=50% and q= 3780W/m^2, the overall heat transfer coefficient was about U=318 W/m^2.C at F=0, U=380 W/m^2.C at F=1.448, U= 362 W/m^2.C at F=2.213. It was also observed that the peak of each curve has been repeated with a comparatively less value when the frequency equals twice the first one.

Effect of the Filling Ratio

Figure 12 shows the variation of the overall heat transfer coefficient (U) with the filling percentage (V^+) at heat flux 3780 W/m^2 ,different dimensionless frequency, and dimensionless amplitude 0.285. The figure shows that the overall heat transfer exists the maximum value at the filling ratio equals 50%. Far from this value, the overall heat transfer coefficient decreases. For example, at q= 3780 W/m^2, B=0.285 and F=1.448, the overall heat transfer coefficient was about U=348 W/m^2.C at V^+=40%, U=366 W/m^2.C at V^+=50%, and U=335 W/m^2.C at V^+=80%.

Effect of the Amplitude

Figure 13 shows the effect of the dimensionless amplitude on the overall heat transfer coefficient at filling ratio 50%, different dimensionless frequency, and at heat flux 3780W/m^2. It is clear that the overall heat transfer coefficient increases with increasing the dimensionless amplitude. The longitudinal amplitude enhances the performance of the thermosyphon by 2.5% to 10.5% over the range of this study.

Correlating the Experimental Data

The present experimental data was correlated in a dimensionless form. This correlation represents the Nusselt number as a function of filling ratio (V^+), Kutatelaze number (Ku), dimensionless frequency (F), dimensionless amplitude (B), and reduced pressure (P/P_{cr}). The empirical heat transfer correlation for vibrated thermosyphon was correlated as:

$$Nu = 2382\ [(V^+)^{-0.252}\ (Ku)^{0.361}\ (1-B)^{-0.244}\ (1-F)^{0.007}\ (P/P_{cr})^{-0.64}] \quad \text{for } V^+ > V^+_{opt} \qquad (5)$$

$$Nu = 3144[(V^+)^{0.254}\ (Ku)^{0.371}(1-B)^{-0.623}(1-F)^{0.0051}\ (P/P_{cr})^{-0.83}] \quad \text{for } V^+ < V^+_{opt} \qquad (6)$$

Where:

Nu Nusselt number, $U\ d_i\ /k_l$

Ku Kutateladze number = $(Q/\pi DL_e/)/(h_{fg}\ [\sigma\ g\ \rho_v^2(\rho_l - \rho_v)]^{1/4})$

V^+ filling ratio

V^+_{opt} optimum filling ratio

F dimensionless frequency. $f\ d_i/\ u_v$

B dimensionless amplitude, $b/\ d_i$

P/P_{cr} reduced pressure

and $1276.2 \le q \le 6331$ W/m^2, $0.3 \le V^+ \le 1.0$, $0.23 \le P/P_{cr} \le 0.3$, $1.08 < F < 3.26$, $0.19 < B < 0.57$

Figures 14 and 15 show the deviation between present experimental data and the present correlation when $V^+ > V^+_{opt}$ and $V^+ \le V^+_{opt}$, respectively. The maximum deviation

between the present experimental data and the present correlation is ± 7.0% and ± 8% respectively.

CONCLUSION

Study of the heat transfer performance of a vibrated two-phase closed thermosyphon tube with R134a as a working fluid is presented. This study is concerned to investigate the effect of heat flux, filling ratio, frequency, and amplitude.

The main results can be summarized as follows:

- The thermosyphon wall temperatures, the operating temperature (corresponding to the operating pressure), the temperature difference between the evaporator and condenser, and the overall heat transfer coefficient are increased by inereasing the input heat flux, over range of this study.
- The optimum-filling ratio is found to be 50%.
- The vibration of the thermosyphon enhances the heat transfer performance by 5 to 18.8% during the case of this study.
- The maximum performance is obtained at the dimensionless frequency value equals 1.448.
- The effect of amplitude on the thermosyphon is slight enhances the heat transfer performance by 5.5 to 10.5 % over range of this study.
- The obtained empirical correlations may be considered a helpful tool for studying the rate of heat transfer from the vibrated thermosyphon. The agreement between these correlations and the obtained experimental results is a quite good.

NOMENCLATURE

b amplitude, mm
d diameter, m
f frequency, Hz
g gravitational acceleration, m/s^2
h convective heat transfer coeff., W/m^2C
h_{fg} latent heat of evaporation, J/kg
k thermal conductivity, W/mC
L length, m
L^* length ratio = L_e/L_c
m mass flow rate, $(m=Q/h_{fg})$
u_v vapor velocity, m/sec
P pressure, bar
q heat flux, W/m^2
Q heat transfer rate, W
T temperature, °C
U overall heat transfer coeff., $W/m^2.°C$
V^+ filling percentage, %

Subscripts

a adiabatic
ave average
c condenser
cr critical
e evaporator
eff effective
i inside
l liquid
op operating
opt optimum
v vapor
0 stationary run

Dimensionless Groups

B Dimensionless amplitude, b/d_l
F Dimensionless frequenvy, $f\, d_i/u_l$
Ku Kutateladze number $=(Q/\pi d_i L_e)/\{h_{fg}[\sigma g \rho_v^2(\rho_l-\rho_v)]^{1/4}\}$
Nu Nusselt number, $U\, d_i/k$
P^* dimensionless pressure, P/P_{cr}

Greek Symbols

σ surface tension. N/m
ρ density, kg/m^3

REFERENCES

1 Lee Y., and Mital U., (1972), A Two-Phase Closed Thermosyphon, Int. J. Heat Mass Transfer, Vol.15, pp. 1695-1707.

2 Imura H., Kusuda H., Ogata J., MiyazakiT., and Sakamoto N., (1979), Heat Transfer in a Two-Phase Closed Thermosyphon, Heat Transfer Japanese Research, Vol.8, No.2, pp.41-57.

3 Nguyen H., Groll M., and Dang-Van T., (1979), Experimental Investigation of Closed Two-Phase Thermosyphon, AIAA, 14th Thermophysics Conference June 4-6, Orlando, Florida, pp.239-246.

4 Shiraishi M., Kikuchi K., and Yamanishi T. (1981), Investigation of Heat Transfer Characteristics of a Two-Phase Closed Thermosyphon, Proceedings of the 4th International Heat Pipe Conference, London, UK, pp. 95-104.

5 Hahne E., and Gross U. (1981) The Influence of the Inclination Angle on the Performance of a Closed Two-Phase Thermosyphon, Proceedings of the 4th International Heat Pipe Conference, London, UK, pp.125-136.

6 Negishi K., and Sawada T. (1983), Heat Transfer Performance on an Inclined Two-Phase Closed Thermosyphon. Int. J. Heat Mass Transfer, Vol.26, No.8, pp.1207-1213.

7 Casarosa, C., Latrofa, E., and Shelginski, A.(1983), "The Geyser Effect in a Two-Phase Thermosyphon", Int. J. Heat Mass Transfer, Vol.26, No. 6, pp.933-941.

8 Gross U., and Hahne E. (1985), Heat Transfer in a Two-Phase Thermosyphon Operating with a Fluid in the Near Critical State, Int. J. Heat Mass Transfer, Vol.28, pp.589-601.

9 Rosler, S., Takuma, M., Groll, M., and Maezawa, S. (1987), "Heat Transfer Limitation in a Vertical Annular Closed Two-Phase Thermosyphon with Small Fill Ratios", Heat Recovery Systems, CHP, Vol. 7, No. 4, pp. 319-327.

10 Faghri, A., Chen, M. M., and Morgan, M. (1989), "Heat Transfer Characteristics in Two-Phase Closed Conventional and Concentric Annular Thermosyphons", ASME Trans. J. OF heat Transfer, Vol. 111, No. 3, pp. 611-618.

11 Negishi, K., Kaneko, K., Matsuoka, T., Hirashima, M., Nishikawa, Y., and Taguchi, M. (1991), "Heat Transfer Performance of a Corrugated-Tube Thermosyphon. Part 1. Evaporator Performance", Heat Transfer Japanese Research, Vol. 20, No. 2, pp. 144-157.

12 Wang, and Ma (1991), " Condensation Heat Transfer Inside Vertical and Inclined Thermosyphons", ASME Trans. J. of Heat Transfer, Vol. 113, No.1, pp. 773-780.

13 Park, R. J., and Lee, Y. (1992), "Two-Phase Closed Thermosyphon with Two Fluid Mixture", Proceeding of the 8th International Heat Pipe Conference, Beijing, China, Vol.2 ,PP. 220-225, September 14-18.

14 Imura, H., Sasaguchi, K., and Kozai, H. (1993), "Critical Heat Transfer in a Closed Two-Phase Thermosyphon", Int. J. Heat Mass Transfer, Vol.26, No.8, pp.1181-1188.

15 Gunnerson F. S., and Zuo Z. J. (1995), Modeling of an Inclined Two-Phase Closed Thermosyphon, ASME / JSME Thermal Engineering Conference, Vol.2, pp. 27-34.

16 Shiraishi M., Terdtoon P., and Murakami M. (1995), Visual Study on Flow Behavior in an Inclined Two-Phase Closed Thermosyphon, Heat Transfer Eng., Vol.16, No.1, pp.53-59.

17 Abdel-Aziz M.(1996), Experimental Analysis of the Optimum Performance of Closed Vertical Thermosyphon Based on Geometry and Liquid Fill Rate Considerations, The 9th Int. Conf. For Mech. Power Eng., (ICMPE.9), Shebin El-Kom, Egypt, December, 21-24.

18 Ferguson, F. T., and Lilleteht, L. U. (1996), " Thermovibrational Convection in a Vertical Cylinder", Int. J. Heat Mass Transfer, Vol. 39, No. 14, pp. 2895-2906.

19 Shiraishi, M., Young, I. K., Murakami, M., and Terdtoon, P. (1996), " A Correlation for the Critical Heat Transfer Rate in an Inclined Two-Phase Closed Thermosyphon", Proceedings of the 5th International Heat pipe Symposium, Melbourne, Australia, pp. 248-254.

20 Terdtoon P., Ritthidej S., and Shiraishi M. (1996), Effect of Aspect Ratio and Bond Number on Heat Transfer Characteristics of an Inclined Two-Phase Closed Thermosyphon at Normal Operating Condition, Proceedings of the 5th International Heat Pipe Symposium, Melbourn, Australia, pp.261-266.

21 Akihiro, S. (1999), "A Flexible Heat Pipe with Carbon Fiber Arterial Wick", 11th

International Heat Pipe Conference – Tokyo, Vol. 1, No. 1, pp.149-159.

22 Hedeaki, I., Kenji, I., and Shigetoshi, I. (1999) " An Experimental Investigation of Geysering in Two-Phase Closed Thermosyphons", 11th International Heat Pipe Conference – Tokyo, Vol. 1, No. 1, pp.166-171.

23 Peterson, G. P., and Ma, H. B. (1999), "Temperature Response of Heat Transport in a Micro Heat Pipe ", ASME Trans. J. of Heat Transfer, Vol. 121, pp. 438-445.

24 Abou-Ziyan, H. Z., Helali, A., Fatouh, M., and Abo El-Nasr, M. M. (2000), "Performance of Stationary And Vibrated Thermosyphon Working with Water And R134a." Proeeeding of 11th International Meehanical Power Engineering Conference, Cairo, Vol. 2, pp. 53-67.

25 Sarhaan H. H. (2000)," Flow and Heat Transfer in Wickless Heat Pipe", Ph.D Thesis, Mansoura University.

26 Shalaby M. A., Araid F. F., Sultan G. I., and Awad M. M. (2000), "Heat Transfer Performance of a Two-Phase Closed Thermosyphon", Proceeding of the 6th International Heat Pipe Symposium, Chiang Mai, pp.269-278.

27 Ong, K. S., and EL-Alahi, M. H. (2000), "Performance of a R134a- Filled Thermosyphon Operating at Low Temperatures", Proceeding of the 6th International Heat Pipe Symposium, Chiang Mai, pp. 244-251.

28 Kim, K. S., Won M. H., Son K. H., Kim H. B., and Han J. S. (2000), Cooling Performance of a Heat Sink With Embedded Heat Pipe, Proceedings of the 6th Int. Heat Pipe Symposium, Chiang Mai, pp.345-351.

29 Murphy K. D., and Lambert T. A. (2000), Modal Effects on the Local Heat Transfer Characteristics of a vibrating Body, ASME Trans., Journal of Heat Transfer, Vol.122, pp.233-239.

30 Melikeyev Y., Prisniakov K., Prisniakov V., Nikolaenko Y., and Kravez Y. (2002), Research a Physical Picture of Heat and Mass Transfer Processes in Vibrating Heat Pipes, 4th Int. Conference on Inverse Problems in Engineering, Rio de Janeiro, Brasil, pp.1-6.

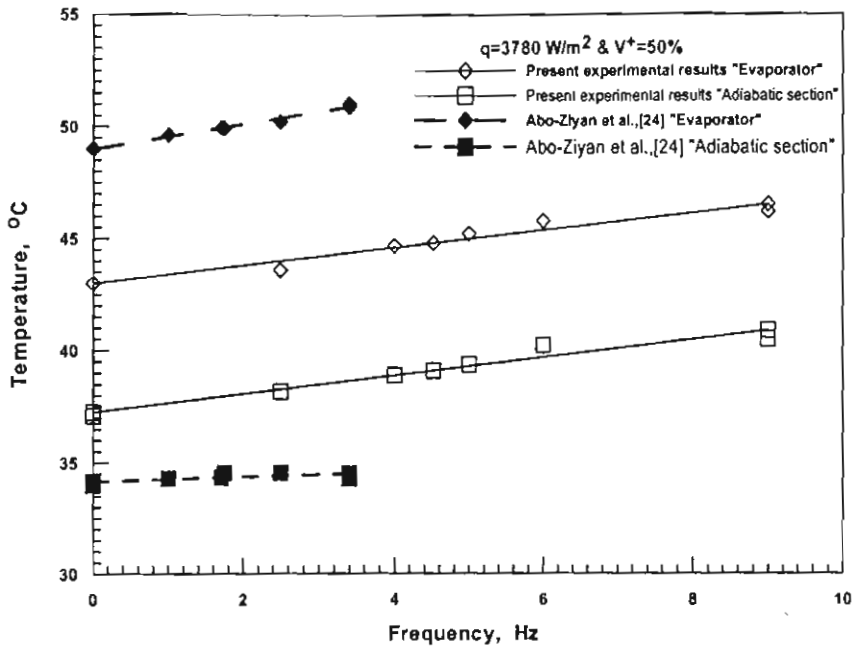

Fig. 3 Comparision of the mean surface temperatur of present experimental results with other.

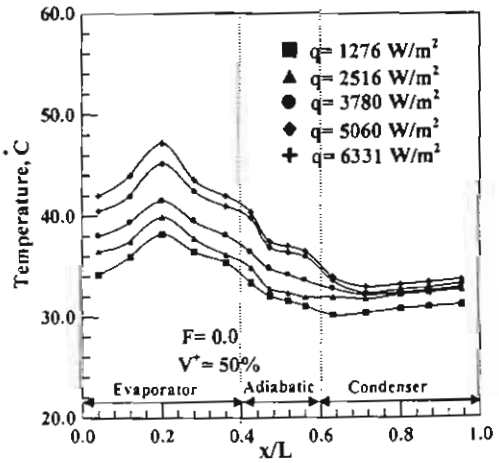

Fig. 4 Temperature distribution along the stationary thermosyphon tube for different values of heat flux and constant of filling.

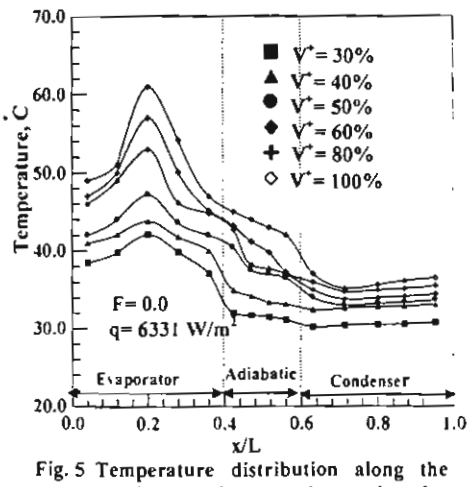

Fig. 5 Temperature distribution along the stationary thermosyphon tube for different values of filling ratio and constant of heat flux.

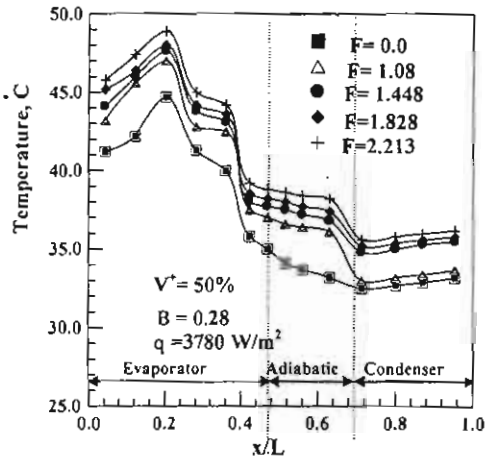

Fig.6 Temperature distribution along the thermosyphon tube for different values of dimensionless frequency and constant of filling ratio, dimensionless amplitude and heat flux

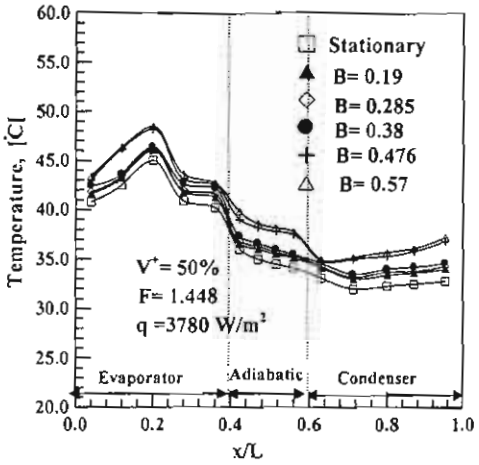

Fig.7 Temperature distribution along the thermosyphon tube for different values of dimensionless amplitude and constant filling ratio, heat flux and dimensionless

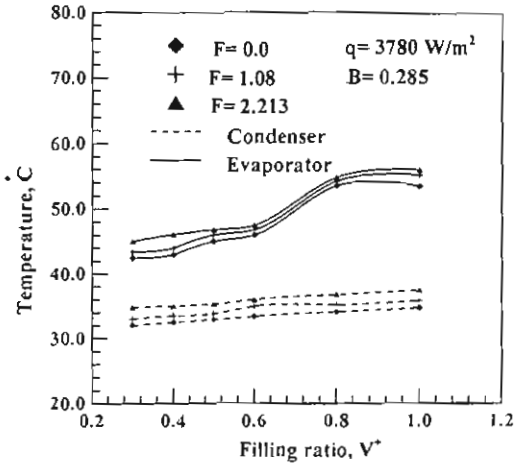

Fig.8 Effect of filling ratio on the average wall temperature of both evaporator and condenser for various values of dimensionless frequency and constant of both dimensionless amplitude and heat flux.

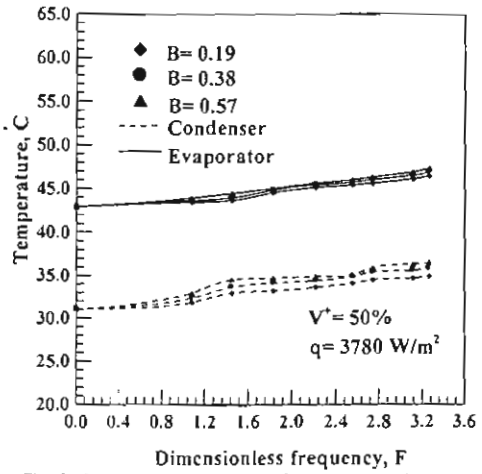

Fig. 9 Effect of dimensionless frequency on the average wall temperature of both evaporator and condenser for various values of dimensionless amplitude and constant of both filling ratio and

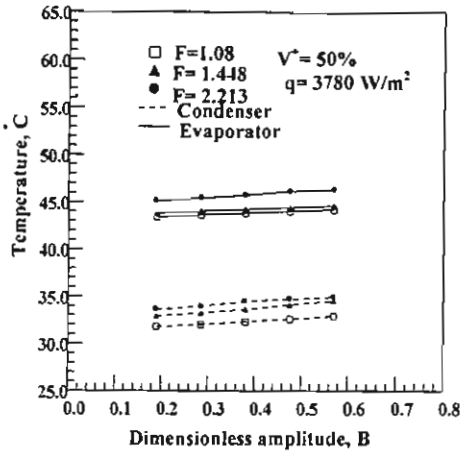

Fig. 10 Effect of dimensionless amplitude on average wall temperature of both evaporator and condenser for various frequencies and constant both filling ratio and heat flux.

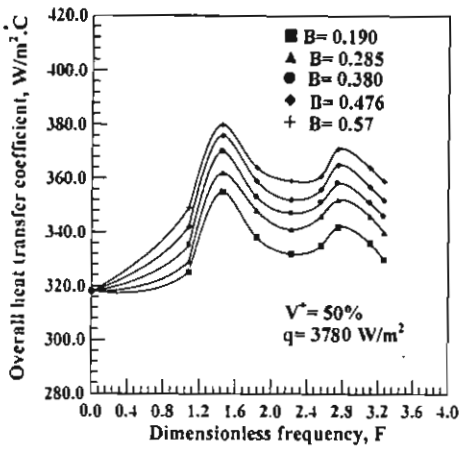

Fig.11 Overall heat transfer coefficient verse the dimensionless frequency at different values of dimensionless amplitude and constant both heat flux and filling ratio.

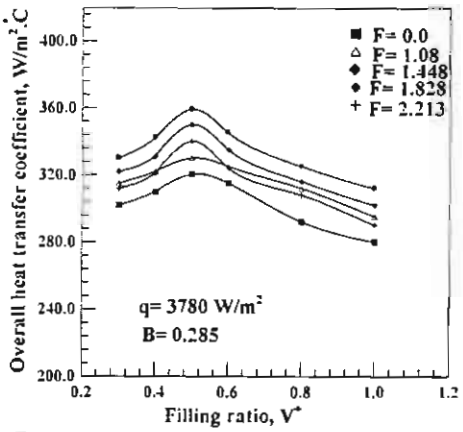

Fig.12 Overall heat transfer coefficient verse the filling ratio at different values of dimensionless frequency and constant both heat flux and dimensionless amplitude.

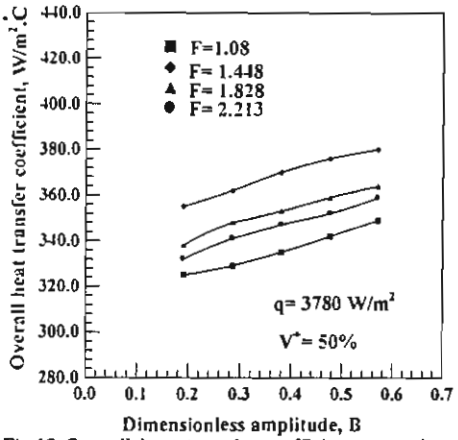

Fig.13 Overall heat transfer coefficient verse the dimensionless amplitude at different values of dimensionless frequency and constant both heat flux and filling ratio.

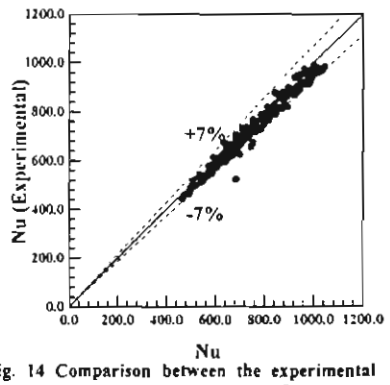

Fig. 14 Comparison between the experimental result and the correlation (Eqn. 5)

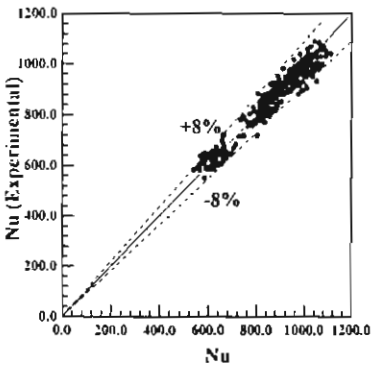

Fig. 15 Comparison between the experimental result and the correlation (Eqn. 6)